Accepted Manuscript

Title: Characterisation of alpha-chitin/poly(acrylic acid) blend

films

Author: Michael Ikpi Ofem

PII: \$2352-9245(17)30037-6

DOI: https://doi.org/10.1016/j.md.2018.01.004

Reference: MD 40

To appear in:

Received date: 4-10-2017 Revised date: 22-11-2017 Accepted date: 13-1-2018

Please cite this article as: { https://doi.org/

This is a PDF file of an unedited manuscript that has been accepted for publication. As a service to our customers we are providing this early version of the manuscript. The manuscript will undergo copyediting, typesetting, and review of the resulting proof before it is published in its final form. Please note that during the production process errors may be discovered which could affect the content, and all legal disclaimers that apply to the journal pertain.



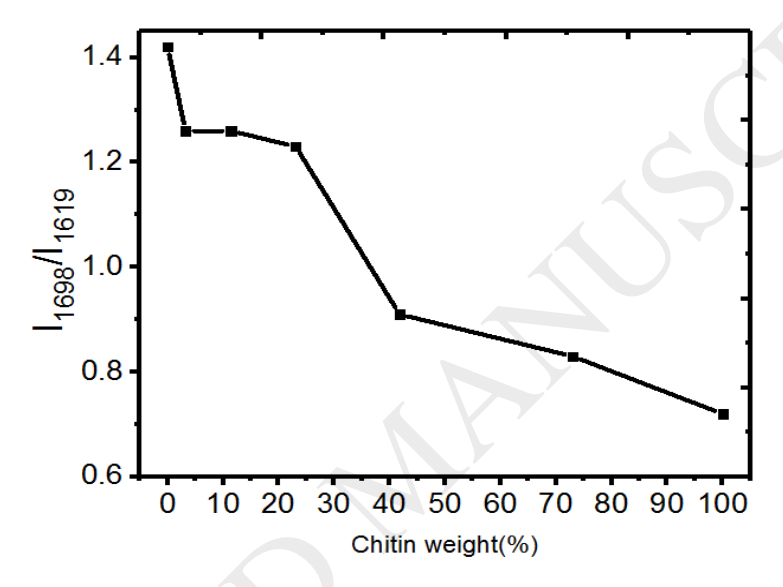
Title: Characterisation of alpha-chitin/Poly(acrylic acid) blend films

Authors: OFEM, MICHAEL IKPI¹

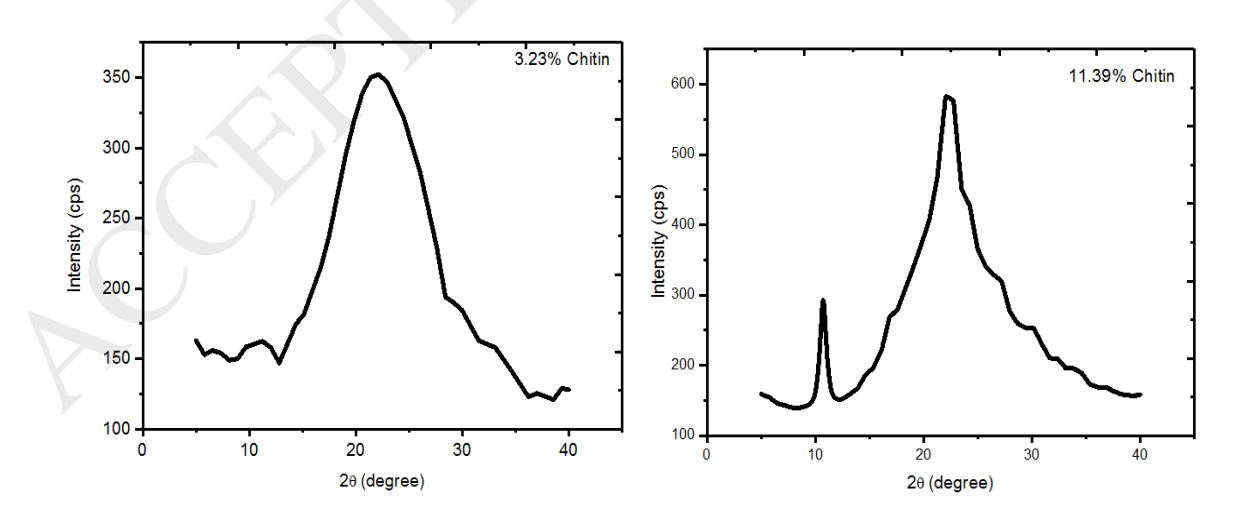
Corresponding Author; Ofem, Michael Ikpi¹ ofemic@yahoo.com

¹Department of Mechanical Engineering Cross River University of Technology Calabar Nigeria

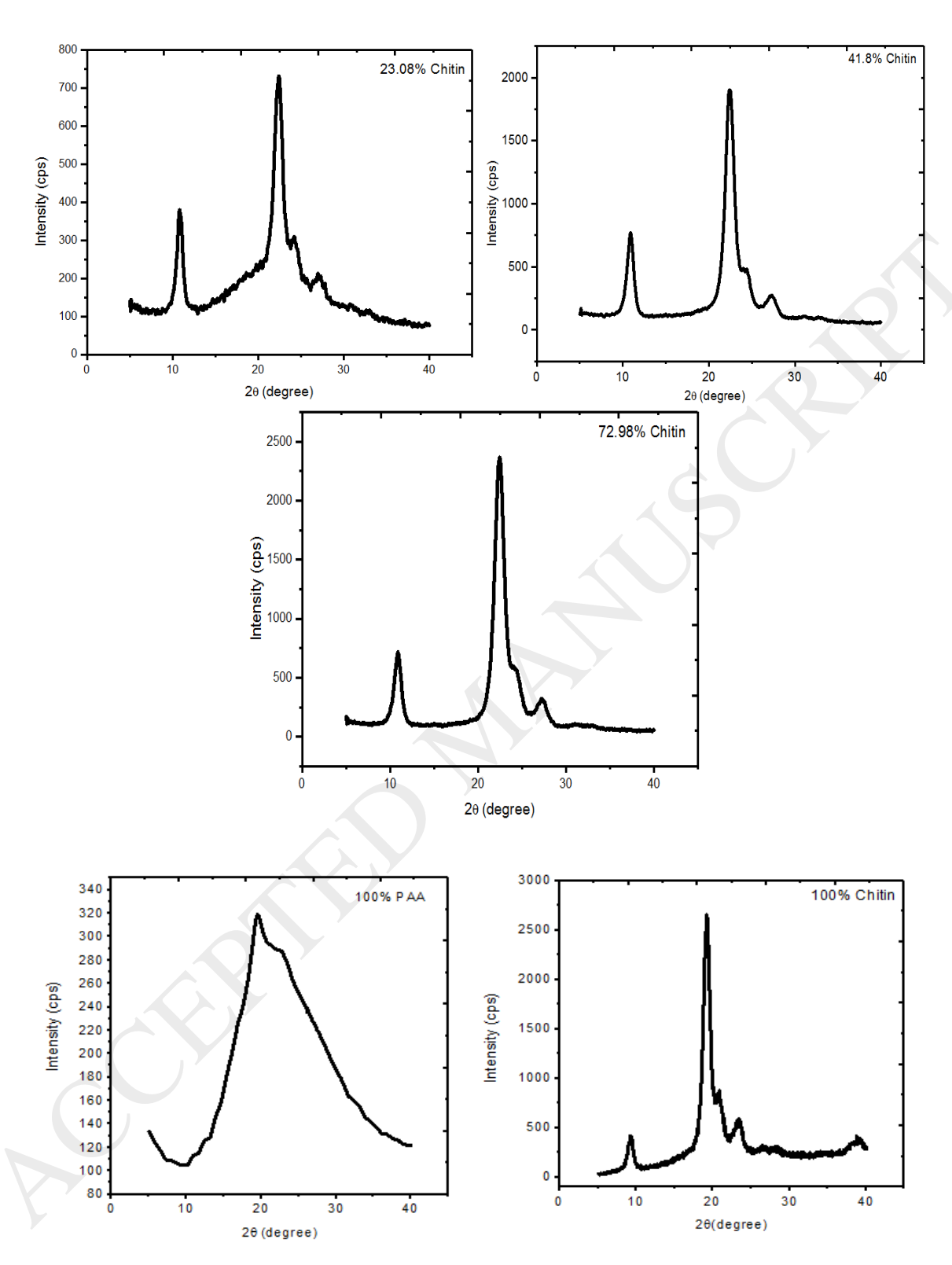
Graphical abstract



The ratio of the intensity of the band absorption at 1698cm⁻¹ to the intensity of the band at 1619cm⁻¹ as a function of Chitin weight.



Page 1 of 19



X-ray powder profiles of chitin, PAA and its composite

Page 2 of 19

Abstract: Chitin whiskers reinforced Poly(acrylicacid) films were prepared by casting. Films were characterised for mechanical and thermal properties. Raman and XRD spectrum and SEM morphology were examined. The tensile strength increased as chitin increases up to 11.39% and gradually decreases. The % strain gradually reduces as whiskers increases. Thermal stability of films improved from those of the pure PAA as the Tg increases at higher whiskers content. The strongest interaction between the carboxylic(C=O) group of PAA and the amide (NH3+) of chitin at the amorphous phase occurs at 3.23% whiskers. The particle size of chitin was reduced as revealed by XRD

Key words: Chitin, Poly (acrylic acid), % chitin, mechanical and thermal properties

1. Introduction

The need to control environmental pollution problems caused by synthetic materials has attracted the research into natural polymer like chitin. It is known in the literature that chitin can be obtained from the exoskeleton of crustaceans, insect cuticle and fungi cell wall (Junkasem, Rujiravanit, & Supaphol, 2006; Morin, & Dufresne, 2002). Bo et al., 2012, isolated chitin in the black coral *Parantipathes Larix* and identified it to be α -chitin. As natural filler, chitin is renewable, biodegradable, biocompatible and available with low density and cost (Tanodekaewa, et al., 2004).

Much effort has been devoted to the use of chitin whiskers as reinforcing agents in polymer (Junkasem, Rujiravanit, & Supaphol, 2006; Morin, & Dufresne, 2002; Junkasem, et al. 2010). As filler, chitin whiskers have shown improvement in the mechanical properties of the matrix. Due to the diameter, the whiskers are almost free from defect. The absence of flaw results in strength that could be close to theoretical value as predicted by the elastic theory (Countney, 1990). This value also depends on the aspect ratio, the interface between the fibre and the matrix and the dispersion of the whiskers in the matrix.

Chitin whisker-graft-polycaprolactone composite using different mixtures of chitin and caprolactone monomer have been formed (Feng, et al., 2009). The report shows an increase in tensile and breaking strength while Young's modulus decreases as the PCL content increased. β -chitin/poly(vinyl alcohol) blend films at different ratios were formed (Peesan *et al.*,2003). The tensile strength was found to increase from 0.7 to 5.1 MPa with an increase in β -chitin content, compared to pure β -chitin or PVA. The percentage elongation at break decreased from 165.2 to 2.9% while the physical appearance of the blend became brittle as the β -chitin content increased.

Both Junkasem et al., (2010) and Junkasem, Rujiravanit, & Supaphol, (2006) used α -chitin as a reinforcement to PVA. Their results show better mechanical properties than Peesan *et al.*, (2003). Gopalan, et al., (2003) carried out chemical modification of crab shell chitin whiskers using three different reagents; namely phenyl isocyanate(PI), alkenyl succinic anhydride (ASA) and 3-isopropenyl-, α , α "-dimethyl benzyl isocyanate (TMI). They investigated the effect of the incorporation of this material into a natural rubber matrix. PI and ASA were used to improve the quality of the interface between the natural rubber used as a matrix and the chitin whiskers, while TMI helped to copolymerize with the natural rubber matrix. The chemical modification resulted in the reduction of the mechanical properties. The decrease in mechanical properties was attributed to the partial or full destruction of the 3D network of chitin whiskers that is assumed to be present in

the unmodified composites.

Despite many reports on chitin-polymer and chitosan-polymer composites, few investigations have been reported for chitin-PAA blend especially at a high percentage of chitin. More so there has been no report on mechanical properties of this composite blend. In this first (deformation of microfibrillated Chitin Film and Composites will be reported) report the properties of Chitin whiskers-PAA blend prepared by solution casting at the different filler loading of whiskers is presented.

2. Experimental

2.1. Materials

Chitin from Shrimp, Poly (acrylic acid) (PAA), $M_W = 250,000~35\%$ wt in H2O and all chemicals were purchased from sigma UK.

2.2 Preparation of blend films

Acid hydrolysis and Purification of chitin were carried out as previously published (Junkasem, Rujiravanit, & Supaphol, 2006; Morin, & Dufresne, 2002; Junkasem, et al. 2010). Chitin whiskers suspension content was approximately 0.3 wt%. Chitin film was fabricated according to a modified earlier published work (Ifuku, et al., 2010; Ifuku, et al., 2011). Purified chitin was roughly crushed with a domestic blender. The crushed chitin was vacuum sieved using a porcelain Buchner filter funnel having an approximate pore of 1.4mm. The sieve chitin was dispersed in water to make 0.5wt% nanofibre content. The pH value was adjusted to 3 by adding few drops of acetic acid. The solution was magnetically stirred overnight at room temperature. The suspension was vacuum filtered. The obtained chitin nanofibre was hot pressed for up to 60 minutes. The temperature was maintained at 80-90°C. Whiskers suspensions and one wt % PAA solution were mixed in a beaker, magnetically stirred at room temperature for about 3-5 min adjusting the pH (which remains at 2 for all samples). The final volume of each solution is maintained at 50ml. The solution was allowed to dry in a plastic Petri dish in a fume hood for 72 hours. The films were later dried in an oven at a temperature of 30°C for about 10 hours. The films were kept in seal bags until when needed.

2.3 Characterisations of films

Raman spectra were collected using Renishaw system 1000 spectrometer which has, a 785 nm near-infrared laser. A TA Q100 heat-flux DSC was used to investigate the thermal properties of the films. Before heating, samples were dried in an oven at a temperature of 70 0 C for 12 hours. Samples were heated at 10 0 C min⁻¹ under 50min⁻¹ nitrogen purge gas flow from room temperature to 250 0 C A NETZSCH Simultaneous Thermogravimetric Analysis instrument was used to characterise the degradation temperature and weight loss. The XRD measurements of films were carried out using X'Pert PW3710MPD, Philips with Cu K α radiation (λ =1.54 Å) with an acceleration voltage of 40KV and current of 30mA. A range of 20 = 5-40 0 was measured at a continuous scan step size of 0.02 and step time of 5s per scan. Instron 1121 tensile testing machine was used to measure the tensile strength and strain. The films were conditioned at 23±3 0 C, 50±5RH for 48 hours, while the gauge length and cross speed were 20mm and 2mm min⁻¹ respectively, an average of between six and nine samples were taken for each composite. A FEM- SEM XL-30 scanning electron microscope operating at a voltage of 10 kV was used to obtain the morphology of films. A JOEL-200FX TEM was used to get the images of the whiskers. The dimensions of CHWs (width and length) for selected images were determined using ImageJ software.

3. Results and discussion

3.1 Morphological properties of CHWs

The prepared whisker suspension exhibited a colloidal behaviour. This response is attributed to the presence of positive charge (NH $^{+3}$) on the whisker surface due to the protonation of amino groups of chitin in an acidic form (Marchessault, Morehead & Walter, 1959). The whisker suspension contained chitin fragment or particles which are slender and rod- like with sharp points (figure 1). The width and length of the whiskers range from 6-49 nm and 62-428 nm respectively. The whiskers are broadly distributed in size. An image analysis was carried out. A total of 230 measurements were taken. The mean width and length were calculated to be 25 ± 11 nm and 233 ± 92 nm respectively. The width has a modal value of 20-29 nm; the length modal class is 200-299 nm. The modal mean width is 25 ± 3 nm while the modal average length is 251 ± 19 nm. The average aspect ratio (L/D; L is the length and D the diameter) is $\approx 9.4\pm8.2$ nm while the modal aspect ratio is $\approx 10\pm2$. These values are smaller to earlier reported values by Morin, & Dufresne, (2002), but agree with Marchessault, Morehead & Walter, (1959); Sriupayo *et al.*, (2005) & Lu, Weng and Zhang (2004) reports. Detailed information of CHWs prepared from different sources of chitins compared to what was obtained here is summarized in table 1

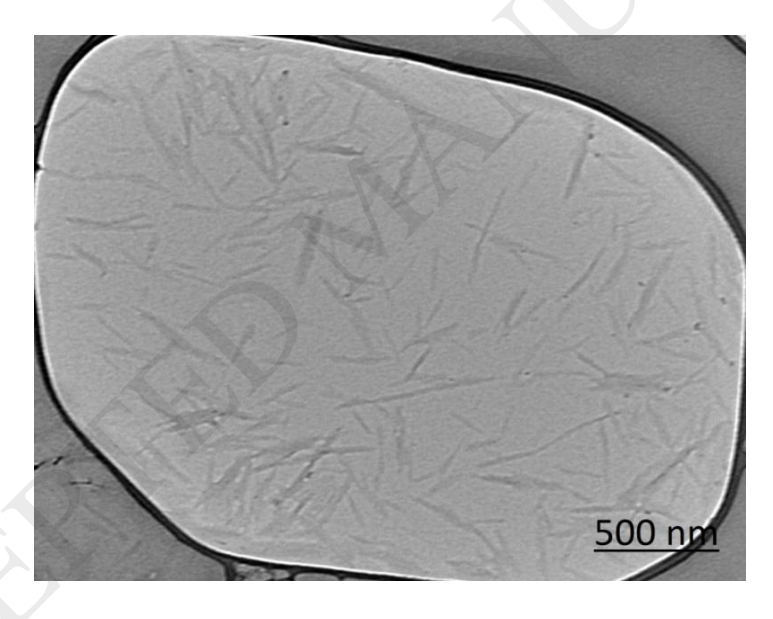


Fig.1. TEM image of CHWs

Table 1 - Sizes, time and temperature of chitin whiskers prepared from different sources of chitin origins

Chitin	(nm)	(nm)	hydrolysis	of heating	g
			(h)	(°C)	
Shrimp	14-36	141-325	1.5	104	This work
Shrimp	12-65	231-969	6	120	Junkasem <i>et al.</i> , [2006]
Shrimp	5-70	150-800	1.5	104	Sriupayo <i>et al.</i> , [2005]
Crab	10-80	100-650	1.5	104	Lu et al., [2004]
Crab	6-8	50-300	1	104	Revol and Marchessault, [1993]
Squid pen	7-70	150-800	1.5	104	Sriupayo <i>et al.</i> , [2005]
Riftia tube	~18	500-10000	1.5	104	Morin and Dufresne, [2002]

3.1 Raman Analysis

Figure 2 Shows the Raman spectra of chitin and PAA and it composites. The band assignment for chitin is based on earlier published literature (Bo, et al., 2012; Cárdenas, et al., 2004; Zia, et al., 2004; Focher, et al., 1992) and for PAA (Peniche, et al., 1993; Dong, Ozaki, & Nakashima, 1997). The single and double H-bonded spectrums which form the basis of amide I band for α-chitin whiskers was split into two at 1656 and 1620cm⁻¹. The 1555cm⁻¹ band is due to NH deformation. The band at 1416, 1376, and 1339 cm⁻¹ are attributed to CH₂ deformation, -CH₃ symmetrical deformation mode and CH₂ wagging respectively. The band at 1269 and 1205cm⁻¹ are mono substituted amide(NH-C-O-CH₃) and amide III respectively while the band at 1109cm⁻¹ is due to C-O-C vibration of chitin-ether and 709 and 650cm⁻¹ are assigned to the OH out- of- plane band and NH(amide) respectively. 1059, 955 and 896cm⁻¹ are respectively C-O stretching, C-O ring vibration and bending. From figure 3B the Raman spectrum of Poly(acrylic acid) at 1% solution is shown. The band at 1456, 1334 and 1102cm⁻¹ are assign to CH₂ deformation, CH₂ twisting and C-CH₂ stretching respectively, while 1698, 841 and 1172cm⁻¹ bands are allocated to C=O and C-OOH stretching vibration of carboxylic groups, C-O stretching coupled with O-H in- plane bending. Other bands are that of 618 and 509cm⁻¹ assigned to CO₂ out of a plane and CO₂ rotation respectively.

A broadband peak is observed for pure PAA at 1698cm⁻¹. This band corresponds to C=O (stretching vibration of the carboxylic acid group). As the chitin content increases, the 1698cm⁻¹ shift to a lower frequency (between 1665 and 1660 cm⁻¹). This is an indication that the intermolecular cyclic dimmer of PAA was gradually replaced with the amino or hydroxyl group of chitin. At 72.98 % chitin, the spectrum was apparently similar to pure chitin as all band associated with pure chitin were found with almost the same frequency but with higher intensity. Equally the CH₂ deformation peak at 1465cm⁻¹ for PAA did not change irrespective of the weight of chitin in the composites, but the Raman intensity decreases as chitin increases.

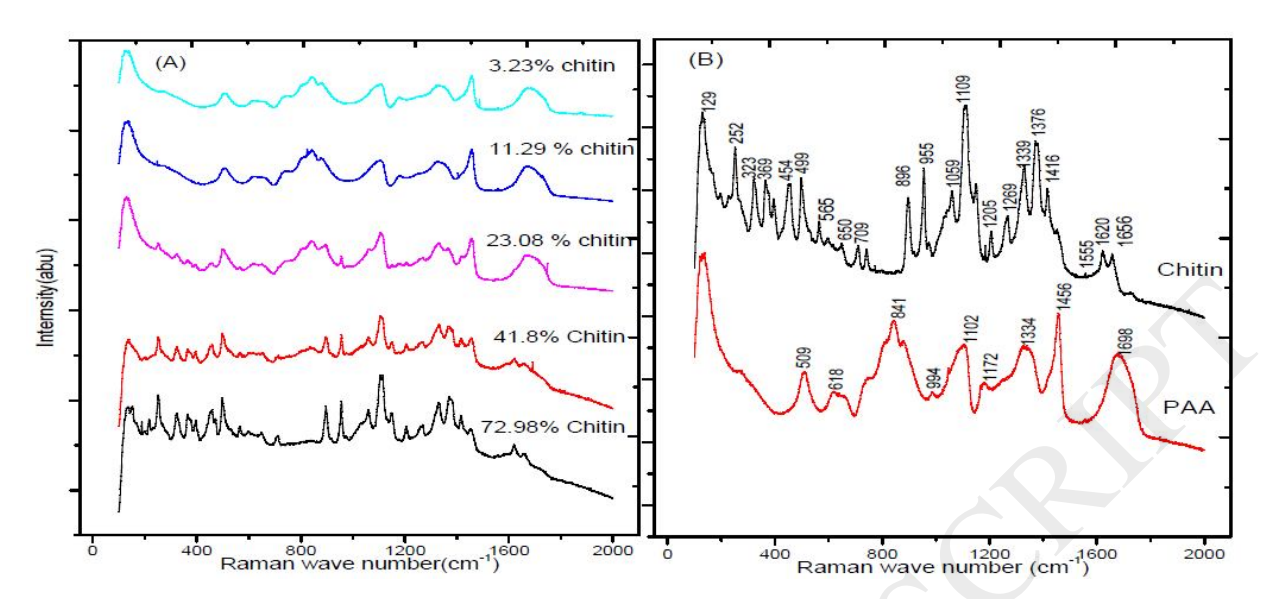


Fig.2. Raman spectra of (A) PAA/Chitin composites films at different chitin content (B) Chitin film and 100 % PAA.

Since the PAA band at 1698cm^{-1} gradually shift to lower frequency towards the amino or hydroxyl group of chitin, this band and 1619cm^{-1} band for chitin were selected to study the interaction between the two polymers as a function of chitin weight in the blend. This has been applied elsewhere (Peniche, et al., 1993; Jeung, & Mishra, 2010). The ratio I_{1698}/I_{1619} of the intensity at 1698 and 1619 cm⁻¹ respectively were chosen, and a graph of ratio vs chitin weight (%) is shown in Figure 3. The intensity ratio decreased by 11% from pure PAA when 3.23% chitin was added. The ratio was almost similar at 11.39 and 23.08% and then dropped by another 26% at 41.8% chitin weight. From the figure, it can be interpreted that the strongest interaction of the carboxylic group in the blend occurs at 3.23% chitin. This interaction gradually reduces as the chitin content increases.

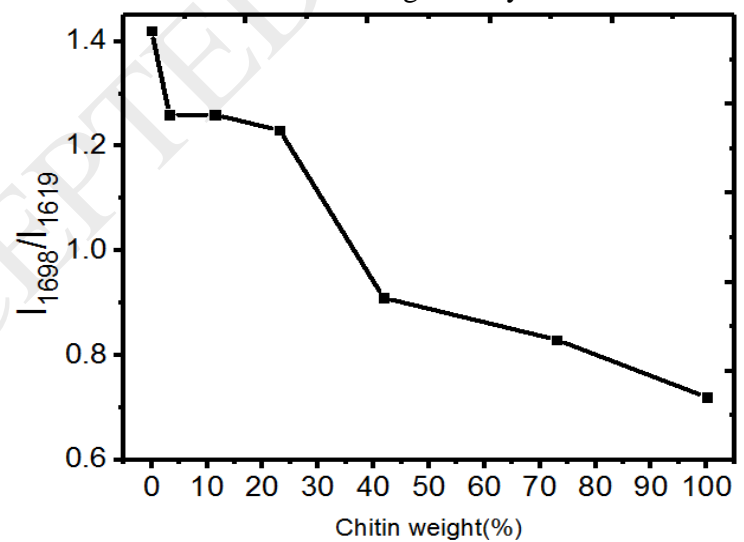


Fig.3. The ratio of the intensity of the band absorption at 1698cm⁻¹ to the intensity of the band at 1619cm⁻¹ as a function of Chitin weight.

3.2 Thermal Properties

Figure 4 shows TGA thermograms of pure PAA, chitin whiskers and its composites at different chitin content. PAA at 1% solution shows a three-stage degradation process. The first weight loss of about 7% occurs within the range 50-162°C which is as a result of water loss and the formation of intra- and inter-molecular anhydride bonds. The second stage degradation which between 217-294 ^oC resulting into a further weight loss of about 26% is related to the decarboxylation process of the anhydride bonds formed in the first stage. A full degradation occurs within the range 362-464 °C and is related to the full degradation of the macromolecule (Tanodekaewa, et al., 2004; Peniche, et al., 1993; Lin, Lee, & Chiu, 2005). Chitin shows two decomposition stages the 1st occurs between 51-80°C which is due to loss of water and the next degradation occurs between 257-391°C, which is the degradation of saccharide rings and the depolymerisation and decomposition of acetylated and deacetylated units of chitin (Peniche, et al., 1993; Kim, et al., 1994). The thermal degradation of the composites as chitin whiskers increases falls between the pure matrix and the filler. As an indication of thermal stability, loss in weight decreases as chitin whiskers increases. The final percentage loss in weight decreases from 81% at 3.23% chitin content to 60% at 72.98% filler. Earlier Dudinsky, et al., (2004) published work shows 55.2% weight loose. The absence of the third stage mass loss at 72.98% filler loading is an indication of none grafting of PAA on the chitin nanofibres.

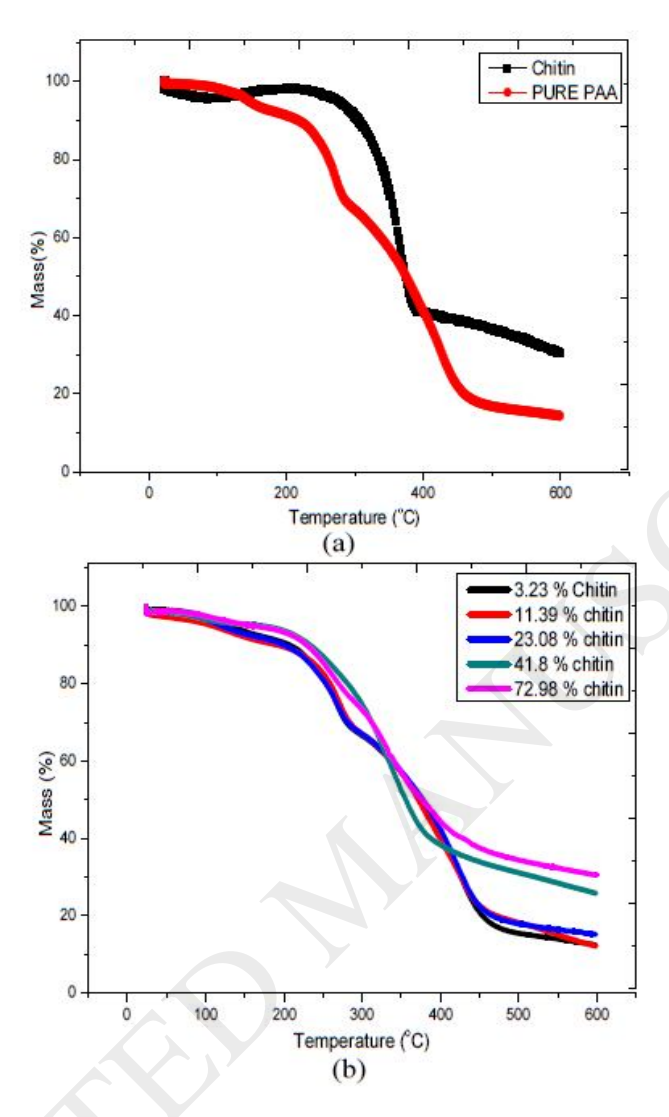


Fig.4. Tga thermo grams of (a) Chitin and Pure PAA and (b) composite at different chitin % loading

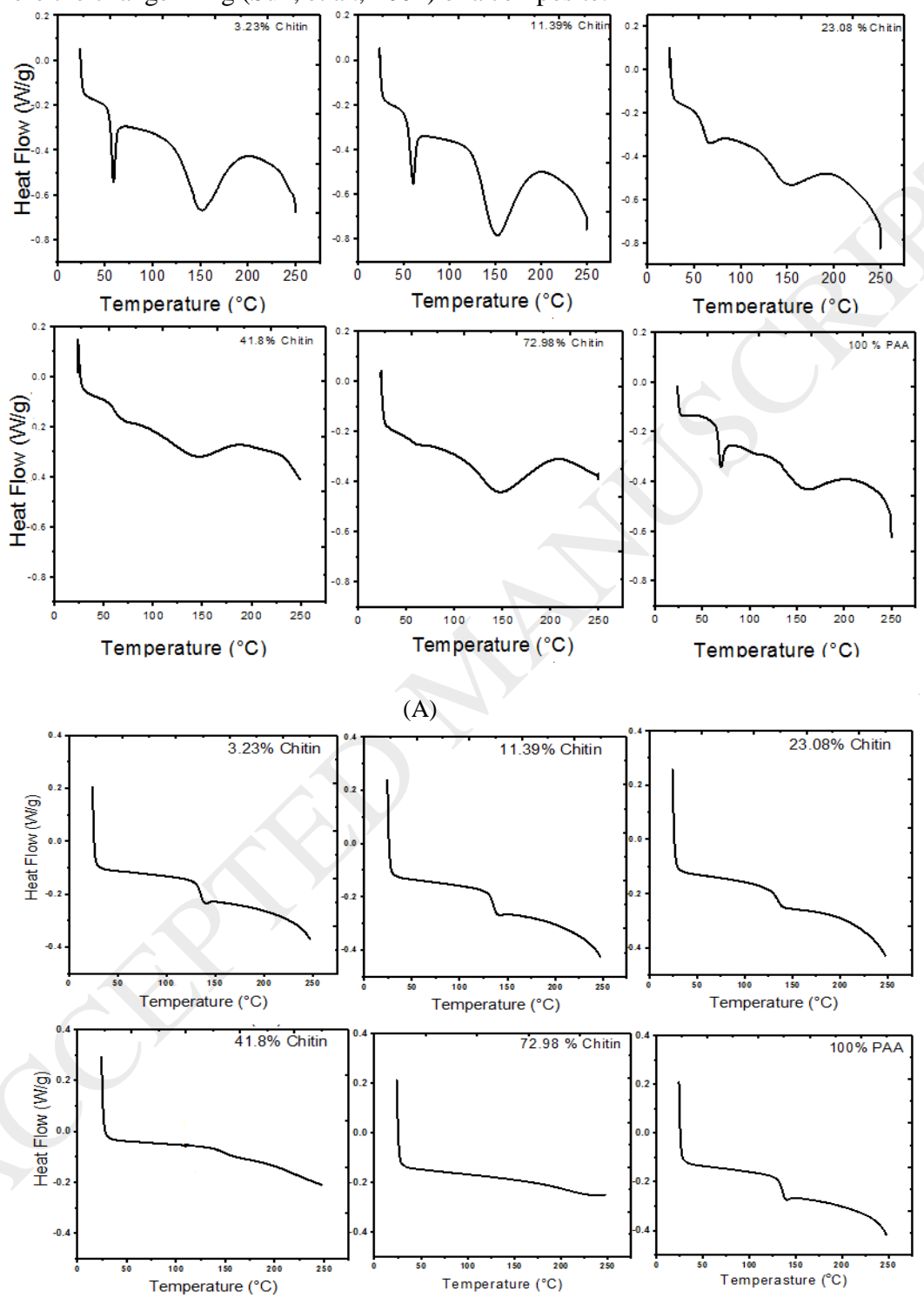
Thermal properties of the composite materials were also characterised using DSC. To investigate the DSC properties both the first and second heating of the filler, matrix and its composites were studied. From Figure 5(C) the thermo gram of chitin homopolymer exhibit an endothermic peak at 135°C, this is attributed to moisture. To eliminate the effect of moisture a second heating was carried out. In the second run, the endothermic peak did not appear confirming that the peak at the first run was a phase transition due to moisture. There has been disparity on the glass transition temperature of chitin. The reasons attributed among other things are, as a natural polymer, the source and or method of extraction can affect the crystallinity, degree of deacetylation and molecular weight of chitin. These properties can invariably affect the Tg of chitin. Some authors (Kittur, et al., 2002; González-campos, *et al.* 2009) in their research could not observe any glass transition, while others (Kim, et al., 1994) reported an apparent relaxation temperature of 509K for α-chitin and evidence of glass transition at 324K was also reported by González-campos *et al.*,

(2009).

Figure 5(A) and (B) shows the DSC profile of glass transition (Tg) of 1st and the 2nd scan of PAA and its composite at different chitin whiskers loading. Like Chitin, there have been wide reported discrepancies in the value of Tg of PAA. Some authors reported it to be between 102-116°C (Maurer, Eustace, & Ratcliffe, 1987; Greenberg, & Kusy, 1980; Eisenberg, Yokoyama, & Sambalido, 1969; Brandrup, & Immergut, 1989; Li, et al. 2007) others between 119-128°C (Dudinsky, et al., 2004; Maurer, Eustace, & Ratcliffe, 1987; Klein, & Heitzmann, 1978). While some reported as has low as 51-79°C (Nam, & Lee, 1997; Fuente, et al. 2005; Smitha, Sridhar, & Khan, 2004; Moharram, & Allam, 2007; Li, et al. 2007) others gave as high as 134-148°C (Eisenberg, Yokoyama, & Sambalido, 1969; Park, Kim, & Kim, 1991; Sun, et al., 2004). The discrepancies depends among other things on, the medium of solvent (Sun, et al., 2004), the molecular weight (Park, Kim, & Kim, 1991) and the drying time and temperature prior to characterisation (Maurer, Eustace, & Ratcliffe, 1987; Sun, et al., 2004). From the 1st scan of Figure 5(A) and (B) a Tg of 56°C and an endodermic peak of 143°C was observed. For the second run, a transparent glass transition at 133°C was also noted. The change in Tg from 56°C to 133°C is a confirmation of dehydration of bound water. Park et al., (1991) reported different Tg values up to 133°C depending on the medium of solvent and the drying temperature and time and Al-Najjar et al.(1996), reported a Tg of 134^oC. In their published work Maurer et al. (1987) and Eisenberg et al., (1969) reported that higher Tg for PAA occurs when there is a formation of anhydride via the intramolecular route. The Tg of PAA at 103°C drying temperature increases as anhydride content increases this resulted into extrapolated Tg of 140°C for linear, pure anhydride when the experimental temperature was 170°C. At 83°C drying temperature FTIR spectrum did not show any anhydride formation, but at 93°C there was traces of anhydride which result into slight increase in Tg(2-5°C). At 103°C and 113°C drying temperature, there was a significant change of Tg up to 120°C. The appearance of FTIR bands at 1806, 1757 and 1030 and the disappearance of bands at 1708 and 1243cm⁻¹ is an indication of the conversion of carboxylic acid to anhydride at a temperature above 93°C. In our Raman spectrum (Figure 3) the bands located at 1698, 509, 618 cm ¹ referring to the vibrational modes in -COOH or -COO- groups were observed. The appearance of this band before characterisation after drying the sample at 70°C for 12 hours indicates that no carboxylic acid was converted to the anhydride. The supplier of this PAA sigma gave a Tg of 106 °C. This Tg was not observed in both the 1st and second run heating of the PAA nor its composites. The absence of this Tg could be attributed to kinetic effects and the weakness of the transition (Eisenberg, Yokoyama, & Sambalido, 1969). It could also be attributed to the ageing of the polymer. Since our sample was dried at 70°C before characterisation at a temperature range of 26-250°C anhydride may have been formed thereby leading to Tg of ≈133°C. The appearance of Tg at 56°C during the first run indicates that our trying temperature and time was not enough to remove the bound water.

As PAA decreases and chitin increases the intensity of the melting endothermic becomes smaller while the melting peaks shift to a lower temperature. From the 1st and 2nd scanning blend the melting peaks of Tg in the blend changes from strong and sharp to weak and broad as PAA decreases. At 72.98% chitin, the Tg peak was almost invisible at the 1st scan and did not appear at the 2nd scan. This shift in Tg could be due to hydrogen bonding and ionic cross-linking of COO of PAA and NH ⁺3of chitin. In a polymer-polymer blend in which one component is crystalline, the mixing of the polymer takes place in the amorphous phase; this results in a decrease in melting

temperature and the suppression of PAA crystallization (Honma, Senda, & Inoue, 2003). Equally the increase or decrease of the interfacial area can influence the polymer chain mobility and therefore the change in Tg (Sun, et al., 2004) of a composite.



Page 11 of 19

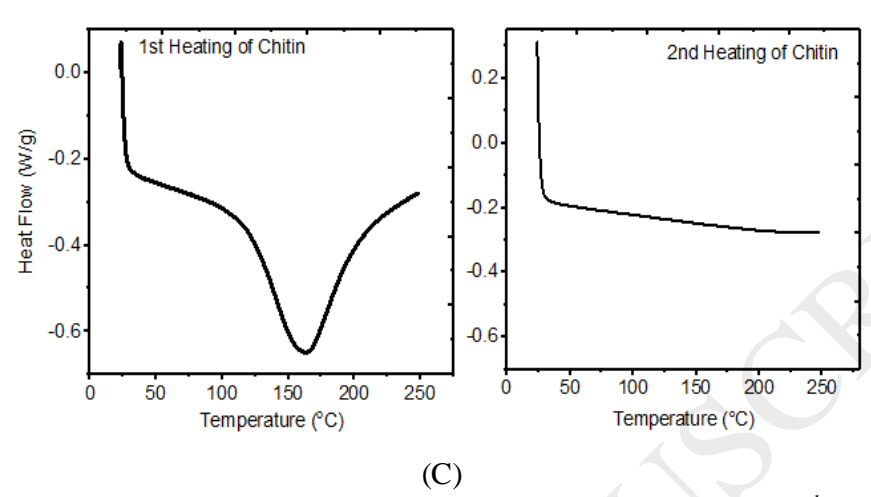


Fig.5. DSC thermo grams of (A) 1^{st} heating of pure PAA and composite (B) 2^{nd} heating of pure PAA and composite and (C) 1^{st} and 2^{nd} Heating of Chitin.

3.1 XRD analysis

In addition to the XRD pattern the crystalline index Icr was calculated from the normalised diffractograms using equation (1) as proposed (Focher, et al., 1990).

$$Crl_{110} = \left\{\frac{I_{110} - I_{am}}{I_{110}}\right\} x \ 100$$

 I_{110} is the maximum intensity of I_{110} peak where $2\theta \approx 19.21$ and I_{am} is the intensity at the amorphous region.

The Debye-Scherrer equation (Zhang, et al.2005). $DI_{110} = \frac{0.9\lambda}{\beta cos\theta}$ was used to calculate the crystalline size.

D = the average crystalline size (Å)

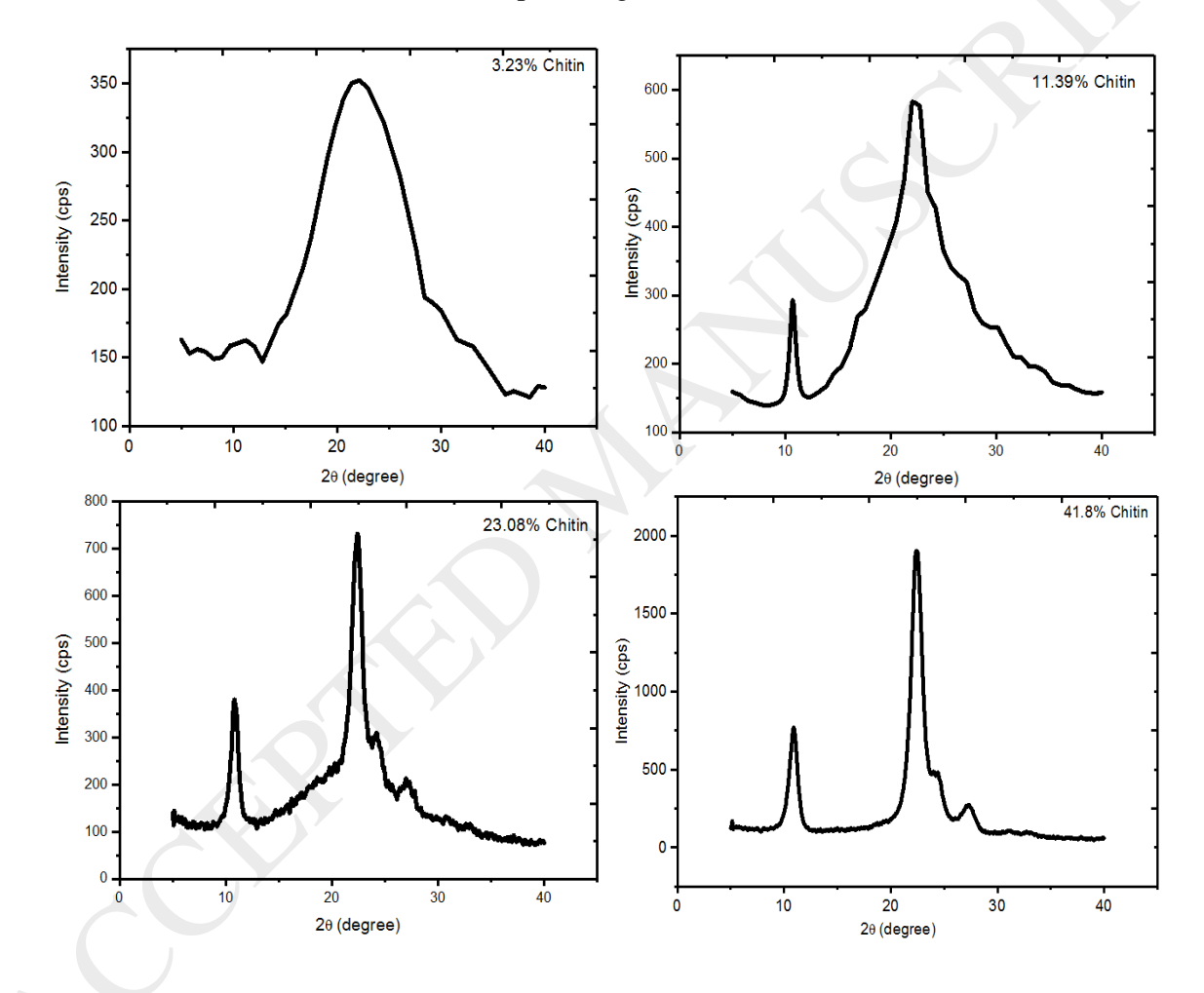
 λ = the wave length (1.54Å)

 θ = Bragg diffraction angle

 β = the full width at half maximum (FWHM) in Radian

By peak fitting of the diffraction profiles, accurate d-spacing was calculated. Figure 6 is the X-ray diffraction patterns of chitin Nanofibres with series of different chitin loading. In the original chitin Nanofibre, the characteristic diffraction peaks of chitin were observed at 9.5° C, 19.21° C, 20.76° C, 23.38° C and 26.62° C; this is typical α -chitin, corresponding to 020, 110, 120, 101 and 130 planes, respectively. These peaks have been observed elsewhere (Kim, et al., 1994; Zhang, et al.2005). Pure PAA shows two peaks at $20\approx 19$ and 22° C. Earlier (Lin, Lee, & Chiu, 2005) results show peaks at between $20\approx 17$ and 22° C. From the figure, all diffraction pattern gradually changes as the filler

loading decreases. The crystalline peak of α -chitin at 19.21°C moved to a higher angle between 22.23 and 22.45°C. Similarly, the peak at 9.50°C for pure chitin moves to a higher angle of between 10.83 and 10.93 °C and finally disappears at 3.23% chitin loading. It is also observed that at 3.23% chitin all characteristics peaks found in pure α -chitin could not be traced. The change in diffraction pattern and peaks as the chitin decreases is an indication of interaction between the filler and the matrix. This interaction is confirmed by the increase in the crystalline index from 61.6% at 3.23% chitin to 92.59% at 100% chitin. The crystalline index of \approx 93% for chitin film is comparable with literature. Cardena et al.,(2004) reported values of between 66.3 and 81.9%. The presence of PAA reduced the particle size of the filler from 4.76nm for 100% chitin to 0.75nm for 3.23% chitin. This reduction in particle size is an indication that the carboxylic acid groups of PAA promoted nucleation and at the same time inhibited particle growth of chitin.



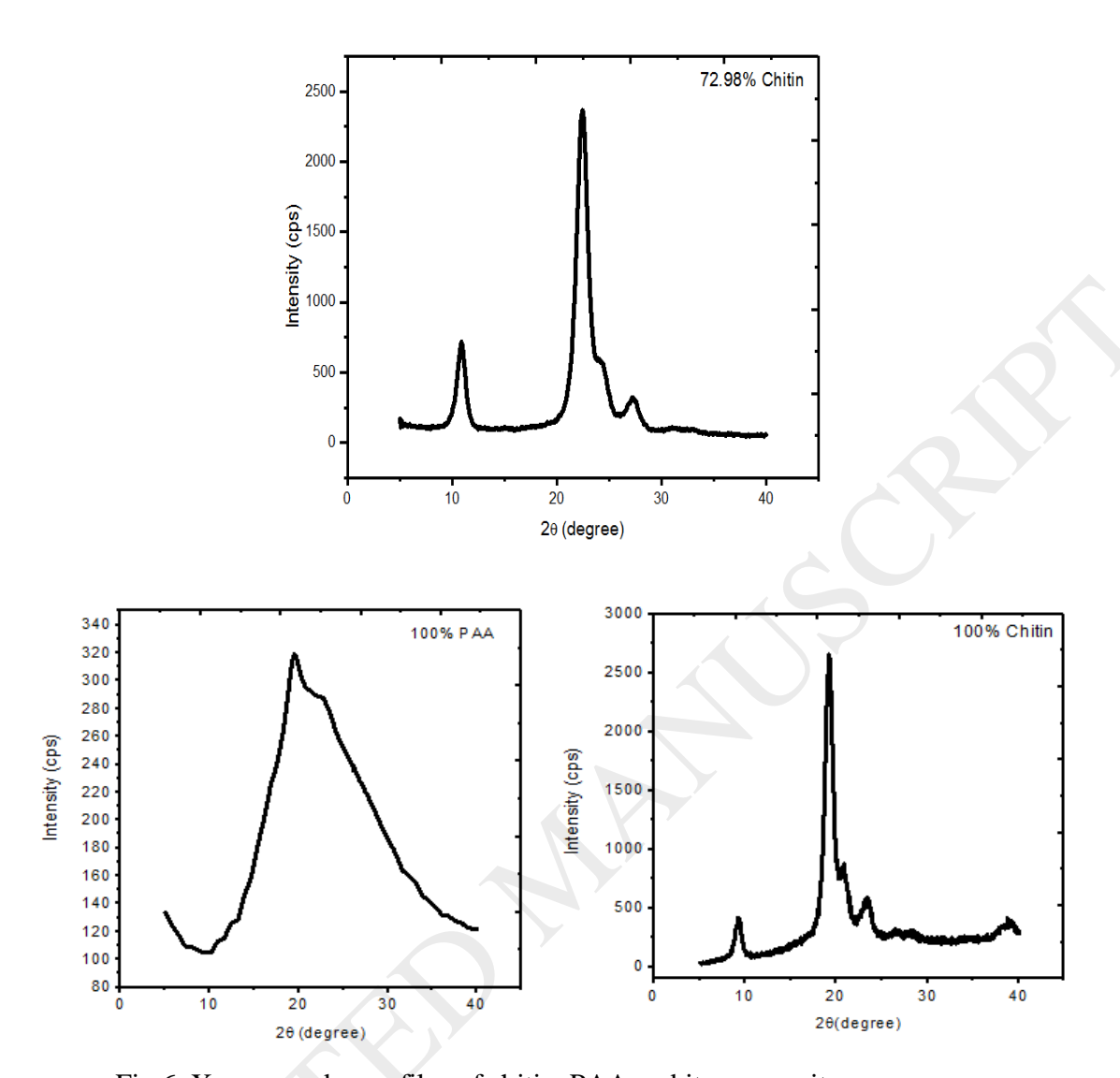
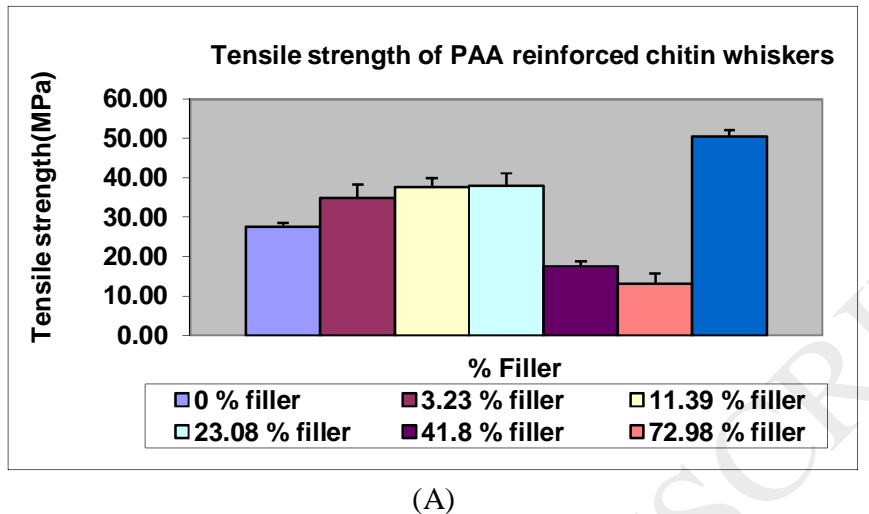


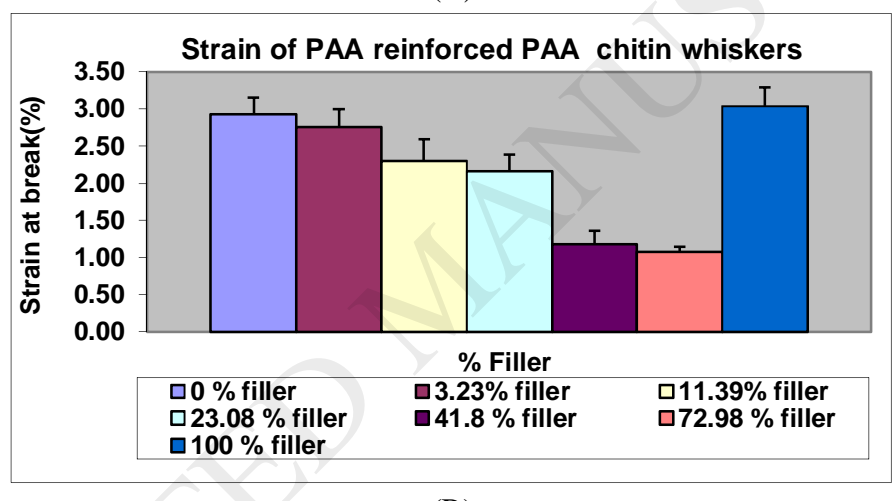
Fig.6. X-ray powder profiles of chitin, PAA and its composite

3.3 Mechanical Properties

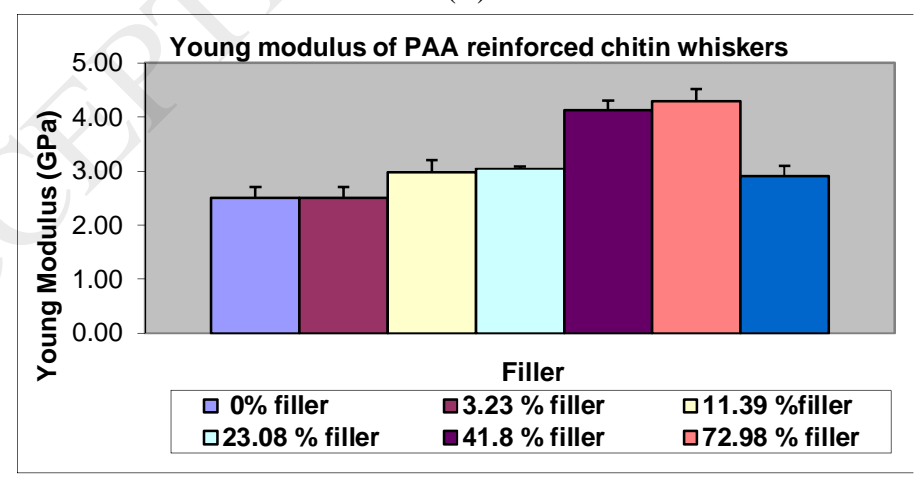
Figure 7 shows the tensile strength, tensile strain and the young modulus of the composites and the respective filler loading (α -chitin whiskers) and matrix (PAA). For the α -chitin film, the tensile strength and percentage elongation at break were found to be $50.41\pm1.57MPa$ and $3.04\pm0.25MPa$ respectively while the tensile strength of PAA and elongation at failure were found to be $27.44\pm1.08MPa$ and $2.93\pm0.22MPa$ respectively. As the filler loading increases, there is an increase in tensile strength up to 11.39% chitin content while the % elongation decreases. The initial increase in strength is attributed to interaction via hydrogen bonding or ionic cross-linking of the polyelectrolyte membranes. During these electrostatic interactions, there is a restriction in mobility, this restriction increases rigidity or strength, thereby reducing the elongation at break. The low tensile strength at higher % chitin content could be attributed to agglomeration of the filler. Due to agglomeration, there is poor interface adhesion between the filler and matrix, this in effect result

into inefficient stress transfer. A similar trend of behaviour have been reported (Junkasem, Rujiravanit, & Supaphol, 2006; Peesan, Rujiravanit, & Supaphol, 2003; Kim et al., 1994).





(B)



(C)

Page 15 of 19

Fig.7. Mechanical properties of Chitin, PAA and chitin whiskers reinforced PAA (a) tensile strength (b) % strain and (c) Young modulus

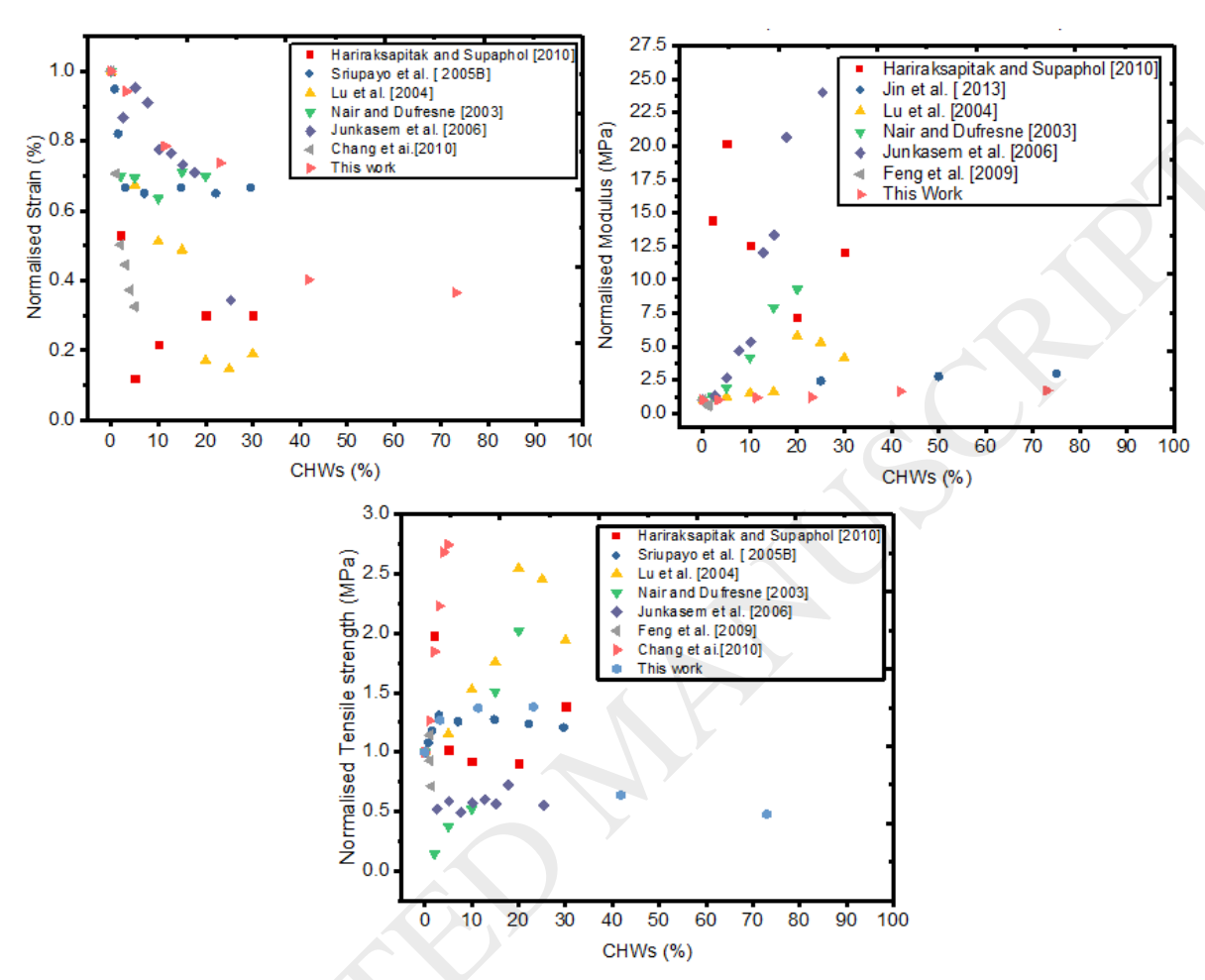


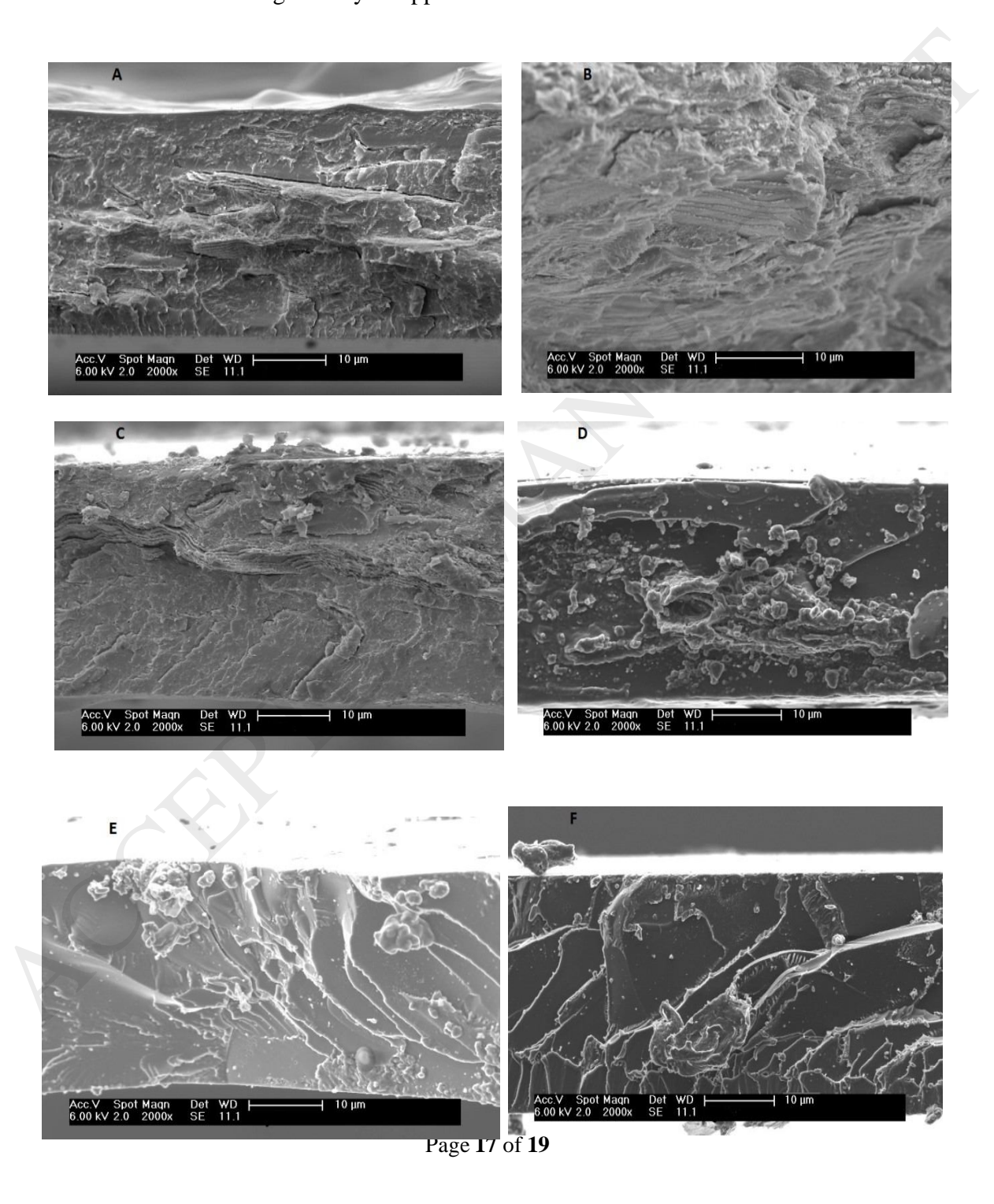
Fig. 8 Normalized (against matrix) Mechanical properties of CHWs reinforced PAA compared with those from literature.

Figure 8 shows the normalized mechanical properties of CHW reinforced polymers composites at different CHW content compared with the result obtained in this report. From the figure there is a clear trend of decrease in strain at break as CHW increases. Most authors agreed that the initial increase in tensile strength and Young's modulus up to a certain filler loading is an indication of strong interactions between whiskers and the matrix. These interactions restrict the motion of the matrix leading to better properties.

3.1 SEM Morphology of Chitin and its Composites

Regardless of the chitin content, all blend consists of randomly aligned standing fibre films. The chitin whiskers appear as white dots and fairly distributed in the matrix at 11.39 % chitin (figure not shown). While uniformly distributed groves were observed at 3.23 % chitin, the groves at 41.8, 23.08 and 11.39 % chitin were not uniform and tend to disappear at 72.98 % chitin and the chitin

film. The coarse surface at some blends indicates that less dispersion of the whiskers. Also, the appearance of nanowhisker-like morphology in the observed blend is an indication of the relative immiscibility of chitin or some level of phase separation. Figure 9 showed fractured surface. PAA fractured surface shows homogenous relatively smooth cross-section devoid of lamellar layers while fractured chitin surface shows rough and thick surface morphology. The relative smoothness of PAA fractured surface gradually disappears to a lamellar surface as the chitin content increases.



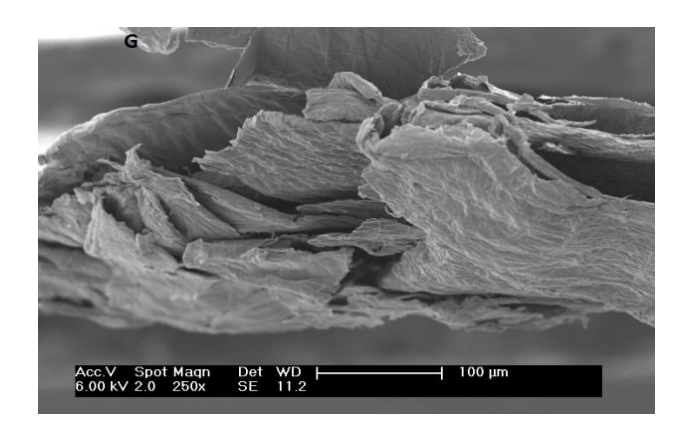


Fig.9. SEM images of (A) 72.98, (B) 41.8, (C) 23.08, (D) 11.39, (E) 3.23 % chitin content (F) PAA and (G) Chitin film fractured surfaces

3 Conclusion

PAA/chitin films of 1% weight PAA and 0.8% chitin whiskers prepared by acid hydrolysis shows efficient stress transfer up to 11.39% chitin content, after which the tensile strength gradually reduces due to a poor interfacial interaction between the matrix and filler. The thermal analysis shows that the endothermic melting peaks Tm and heat of fusion ΔH_f loses prominence and decreases indicating the depression of PAA crystallite. The Tg of the blend did not increase monotonically as chitin increases but assume a maximum at 23.08% and 41.8% chitin during the first and second heating respectively. This difference indicates that internal stress, orientation effect and absorbed water during storage may have affected the Tg during the 1^{st} scan.

References

- 1. Junkasem J, Rujiravanit R. and Supaphol P. Nanotechnology, 17(2006), 4519-4528.
- 2. Morin A and Dufresne A. Macromolecules, 35(2002)2190-2199
- 3. Bo M, Bavestrello G et al,. International Journal of Biological Macromolecules. 51(2012) 129-
- 4. Tanodekaewa S, Prasitsilpa M, Swasdison S, Thavornyutikarn B, Pothsree T and Pateepasen R. Biomaterials 25 (2004) 1453-1460
- 5. Junkasem J., Rujiravanit R., Grady B.P. and Supaphol P. Polymer International, 59(2010), 85-91.
- 6. Countney T H In Mechanical Behavoiur of materialsMcGraw Hill New York 1990, pg 83
- 7. Feng L, Zhou Z, Dufresne A, Huang J, Wei M and An L: Journal Of Applied Polymer Science 2009;112:2830-2837
- 8. Peesan M, Rujiravanit R, and Supaphol P. Polymer Testing, 22 (2003), 381-387
- 9. Gopalan Nair K, Dufresne A, Gandini A, Belgacem M. Biomacromolecules. 2003 Nov-Dec; 4(6):1835-1842
- 10. Ifuku S, Nogi M, Yoshioka M, Morimoto M, Yano H and Saimoto H. Carbohydrate Polymers 81 (2010) 134-139
- 11. Ifuku S, Morooka S, Nakagaito A, Morimoto M and Saimoto H. Green Chem. 13(201) 1708-1711
- 12. Show-An Chen and Hsun-Tsing Lee. Macromolecules 28(1995) 2858-2866
- 13. Marchessault RH, Morehead RR and Walter NM. Nature. 1959; 184:632-633.
- 14. Sriupayo J, Supaphol P, Blackwell J and Rujiravanit R. Polymer 2005; 46:5637-5644.
- 15. Lu Y, Wend L and Zhang L. Biomacromolecules 2005; 5:1046-1051.

- 16. Cárdenas G, Cabrera G, Taboada E, Miranda S P. J Appl Polym Sci. 93(2004) 1876–1885.
- 17. Zia K M, Barikani M, Zuber Ijaz M, Bhatti A and Sheikh M A. Carbohydrate Polymers 74(2004) 149-158
- 18. Focher B, Naggi A, Torri G, Cosani A and Terbojevich M. Carbohydrate Polymer 17(1992) 97-102.
- 19. Koda S, Nonura H and Nagasawa M. Biophysical Chemistry 15 (1982) 65-72
- 20. Dong J, Ozaki Y and Nakashima K. Macromolecules 30(1997)1111-1117
- 21. Peniche C, Argüelles-Monal W, Davidenko N, sastre R, Gallardo A, Romàn J.S. Polym Sci: Part A: Polym Chem, 31 (1993), 485-491
- 22. Jeung S, and Mishra M K. International Journal of Polymeric Materials and Polymeric Biomaterials, 60(2010), 102-113
- 23. Lin C, Lee C and Chiu W. Journal of Colloid and interface Science 291 (2005) 411-420.
- 24. Kim S, Kim S, Moon Y and Lee Y. Polymer 35(1994) 3212.
- 25. Dudinsky S, Grader S, Shter G, Silverstein M. Polymer Degradation and Stability 86 (2004) 171-178
- 26. Kurita K, Inoue M and Harata M. Biomacromolecules 3(2002) 147-152
- 27. Kittur F, Prashanth K, Sankar K and Tharanathan R. Carbohydrate Polymer 49(2002) 185-193
- 28. González-campos J, Prokhorov E *et al* . Journal of Polymer Science Part B: Polymer Physics, 49(2009) 932-943
- 29. Maurer J, Eustace D and Ratcliffe C T. Macromolecules 20(1987) 196-202
- 30. Greenberg, A. R.; Kusy, R. P. J. Appl. Polym. Sci. 1980, 25, 1785-1788
- 31. Eisenberg A, Yokoyama T and Sambalido E. Polym. Sci., Part A-I (7)19691717-1728
- 32. Brandrup J and Immergut E, Eds.; Polymer Handbook, 3rd Ed., Wiley: New York, 1989 chapter 6
- 33. Klein J, Heitzmann R. Makromol. Chem. 179(1978) 1895-1904
- 34. Nam S and Lee Y. Journal of membrane Science 135(1997) 161-171
- 35. Fuente J, Wilheilm M, Spiess H et al . Polymer 46(2005) 4544-4553
- 36. Smitha B, Sridhar S and Khan A. Macromolecules 2004; 37:2233-2239.
- 37. Moharram M. A. and Allam A. M. Journal of Applied Polymer Science, 105(2007),3220-3227
- 38. Li B, Xu L, Wu Q, Chen T, Sun P, Jin Q, Ding D, Wang X, Xue G and Shi A. Macromolecules, 40(2007), 5776-5786
- 39. Park J, Kim D and Kim C. Polymer Engineering and science 36(1991) 867-872
- 40. Sun Y, Zhang Z, Moon K and Wong C P. Journal of Polymer Physics 42(2004) 3849-3858
- 41. Honma T, Senda T and Inoue Y. Polymer International Polym Int. 52(2003),1839-1846
- 42. Sun Y, Zhang Z, Moon K and Wong C P. Journal of Polymer Physics 42(2004) 3849-3858
- 43. Focher B, Beltranme P, Naggi A and Torri G. Carbohydr Polym. 12(1990)405-418.
- 44. Zhang Y, Xue C, Xue Y, Gao R and Zhang X. Carbohydrate Research 340 (2005) 1914–1917